


Article

Balancing Hazard Exposure and Walking Distance in Evacuation Route Planning during Earthquake Disasters

Wonjun No , Junyong Choi, Sangjoon Park and David Lee *

Department of Civil and Environmental Engineering, Korea Advanced Institute of Science and Technology (KAIST), 291 Daehak-ro, Yuseong-gu, Daejeon 34141, Korea; jn0704@kaist.ac.kr (W.N.); wnsdyd@kaist.ac.kr (J.C.); psj1866@kaist.ac.kr (S.P.)

* Correspondence: david733@kaist.ac.kr; Tel.: +82-42-350-5677

Received: 30 May 2020; Accepted: 7 July 2020; Published: 10 July 2020



Abstract: Efficient evacuation planning is important for quickly navigating people to shelters during and after an earthquake. Geographical information systems are often used to plan routes that minimize the distance people must walk to reach shelters, but this approach ignores the risk of exposure to hazards such as collapsing buildings. We demonstrate evacuation route assignment approaches that consider both hazard exposure and walking distance, by estimating building collapse hazard zones and incorporating them as travel costs when traversing road networks. We apply our methods to a scenario simulating the 2016 Gyeongju earthquake in South Korea, using the floating population distribution as estimated by a mobile phone network provider. Our results show that balanced routing would allow evacuees to avoid the riskiest districts while walking reasonable distances to open shelters. We discuss the feasibility of the model for balancing both safety and expediency in evacuation route planning.

Keywords: evacuation route planning; disaster mitigation planning; GIS-based decision support systems for risk analysis and emergency management

1. Introduction

Serious earthquakes in 2016 and 2017 brought public attention to the need for emergency response and proactive disaster planning in South Korea. The 2016 Gyeongju earthquake damaged 5868 facilities and required 117.94 million USD for the recovery of parts of the city [1]. Efficient evacuation planning is an essential strategy in earthquake disasters to allow quick escape from hazard zones and navigate citizens to safe shelters. The South Korean government categorizes emergency shelters into temporary and permanent shelters [2]. Temporary shelters protect people from immediate harm when disasters happen and can be any open spaces such as small parks or parking lots distant from hazards.

By contrast, citizens must evacuate to permanent shelters in the moments following an earthquake. These are seismic-designed buildings that have sufficient space to accommodate citizens for hours or days, while the city assesses the damage and ensures that it is safe to return home. Permanent shelters are selected by local governments and are usually large public buildings such as schools or community centers. Since roads in dense building environments may become congested or blocked by debris following an earthquake, permanent shelters must be accessible by foot for the majority of users.

In earthquake disasters, it is important to quickly navigate citizens to the shelters. Any individual person's ability to find the best evacuation route will be limited if they lack information, such as which roads will be dangerous and which shelters will be fully occupied [3,4]. Evacuation route plans

assign evacuees to fixed shelters and routes before disasters, to avoid chaos and increase evacuation efficiency [5,6].

Geographical information systems (GIS) are commonly applied to generate evacuation routes through pedestrian path networks. Most approaches select routes using a shortest path calculation that chooses the minimum distance from residences to shelters [5–7]. However, shortest path calculations do not take into account the fatal risks that pedestrians might experience while they walk in hazard zones. Previous studies have identified potential risks while evacuating, such as building collapse, flooding, and toxic gas [8,9]. Others have attempted to incorporate safety indicators into evacuation route analysis in disaster situations [10–15]. These studies estimated hazard zones and identified roads traversing these hazard areas in disaster situations. [12–15]. However, they focused on evaluating the existing shortest paths to shelters, rather than calculating new routes that prioritized pedestrian safety [10–15]. In addition, previous research used simulated populations [14] or census-based residential population distributions [11–15] that did not reflect the actual locations of people at different hours of the day. Thanks to the development of locative technologies such as mobile phone network and GPS tracking, we can retrieve floating population distributions and create evacuation plans in real-time.

Current research has focused on balancing safety and distance in evacuation planning [16–18]. These studies attempted to improve upon previous approaches that only minimized travel time to save citizens in disaster situations. They had two common objectives when judging evacuation routes: (1) risk assessment to estimate road hazards in disasters and use them as travel costs while traversing the road network, and (2) route analysis to find the best route along with the shortest distance and minimal risk. The risk of hazard exposure was converted to costs for routes delaying or inhibiting pedestrian movement [16,17]. The suggested routes were generally longer than the shortest paths determined by Dijkstra's algorithm [19], but they diminished the injuries and fatalities of pedestrians in disaster situations. The optimization rules to find the shortest safe path depended on the priority and weight of the objectives, and researchers have attempted to balance walking distance and hazard exposure for the best evacuation route planning.

In this study, we propose a new evacuation route assignment model that considers potential road hazards in earthquake disasters. We have three objectives in this study: (1) to estimate the potential road hazards from building collapse, (2) to calculate evacuation routes through heuristic route analysis that minimize hazard exposure and walking distances, and (3) to compare the efficiencies of routes with those determined by other methods such as the shortest path method. We applied our approaches to geospatial data covering the urban core of Gyeongju, South Korea. The rest of this paper is structured as follows:

1. Materials and methods: overview of our study site and spatial dataset, and methods of road hazard estimation and pedestrian evacuation route analysis.
2. Experimental results: visualization of resulting routes.
3. Discussion: discussion of results and limitations.
4. Conclusion: summary of the study and directions for future work.

The main contributions of this paper are as follows: Firstly, we present our computational method for evacuation route planning, quantitatively incorporating road hazards from building collapse as pedestrian safety risks in earthquake disasters. Secondly, we demonstrate how these routes can be generated and optimized for individuals throughout a city based on their real-time locations, as determined from floating population estimates from mobile phone networks.

2. Materials and Methods

2.1. Data Sources

In this study, we used data from Gyeongju city, South Korea, the site of a major and destructive earthquake in 2016. Gyeongju is located in the southeastern region of South Korea, near important industrial cities such as Pohang, Ulsan, and Daegu. This region has suffered from earthquake disasters in recent years. An earthquake of M_L 5.8 hit Gyeongju on 12 September 2016, and an earthquake of M_L 5.4 hit Pohang on 15 November 2017 [20]. In particular, the Gyeongju earthquake was the largest one recorded in South Korea since measurements were started [21]. Since 2017, 211 earthquakes between M_L 2 and M_L 4 have occurred in the inland areas of South Korea; 78% (164) hit this southeastern region of Korea [22]. These disasters threaten the core industries of the region: steel, shipbuilding, automobiles, and chemicals.

Gyeongju itself has many historical districts, and their historic structures are vulnerable to damage or collapse in earthquake situations. In addition, although the Korean government has strengthened the seismic design regulations for new buildings, many buildings in the central districts of Gyeongju predate these rules and are vulnerable to earthquake disasters. Despite it being a small city, Gyeongju's vulnerability to earthquake disasters reflects on the danger to many small and large cities in the region, with economic and social consequences for the nation.

We used several spatial datasets, along with floating population data from a mobile phone provider. We used the following spatial datasets: (1) road network (linestring layer), (2) buildings (polygon layer), and (3) permanent shelter locations (point layer). We used a road layer [23] that captures the center lines of vehicle roads as potential pathways for evacuation. We transformed the road layer into a network graph $G(N, E)$ consisting of edges (E) representing paths and nodes (N) wherever two or more edges meet. Our building layer represented building roof contours as polygon features, which included the number of floors in their attributes [24]. Permanent shelter locations were provided by the local government [25], and consisted of 20 public schools; their attributes included facility areas.

The mobile phone data collected by SKT, the nation's largest mobile network company, inferred residents' activities based on mobile phone usage patterns [26]. They came in the form of anonymized, estimated population distributions within a $50\text{ m} \times 50\text{ m}$ grid. The data for the mobile phone activities for an hour were aggregated, and the population distributions within each grid cell in that hour were estimated. We converted the data into a polygon layer of $50\text{ m} \times 50\text{ m}$ square features.

In this study, we observed 127,867 people present in 4808 grid cells of Gyeongju's urban core, at 8 p.m. on 12 September 2016 (the hour at which the earthquake occurred) (Figure 1). The residential population of the study site was estimated at 118,992 in December 2016 [27]; the floating population was estimated to be 7% larger than the residential population at the exact moment of the earthquake. Many tourists visit Gyeongju and stay in hotels and guesthouses in the central districts of the city. The mobile phone data imply that floating populations might significantly diverge from residential populations in historical and tourist cities and should be factored into evacuation plans based on where people are. The collection of floating population data coinciding with a major earthquake presents a unique opportunity to test our ideas for disaster management in South Korea.

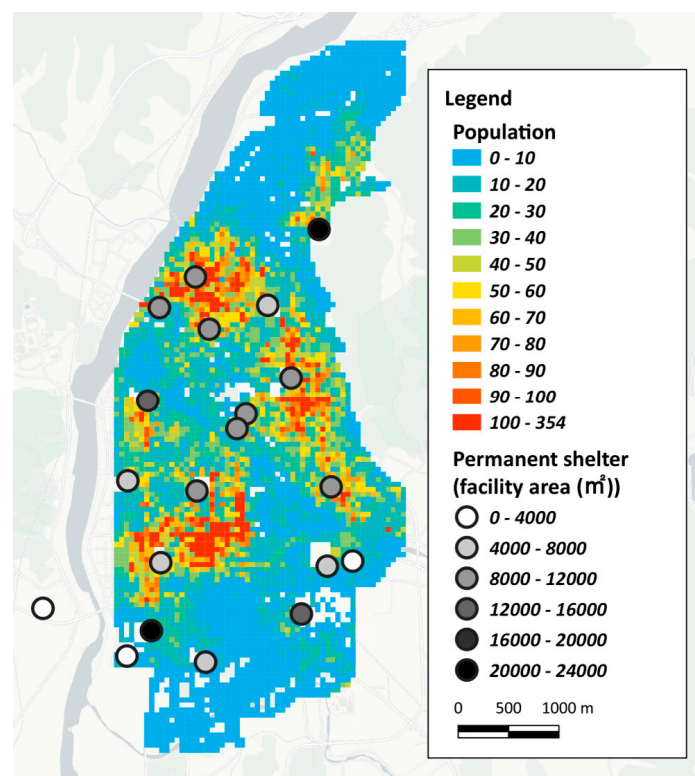


Figure 1. Population distribution at the time of the earthquake, and permanent shelter locations in Gyeongju. People are mostly concentrated in three main districts in the city.

2.2. Building Collapse Estimation and Road Hazard Analysis

In this section, we describe how we accounted for potential road hazards from building collapse in earthquake disasters.

Building collapse is the most fatal risk for pedestrians while they evacuate to shelters [14]. Falling debris or debris on roads could harm or block pedestrians [28]. South Korea's Building Act has revised seismic design regulations to protect buildings from wind pressure, vibrations, excitations, and collapse in disaster situations from 1990 to 2018. In particular, the Building Act has been frequently revised since the major earthquakes in 2016 and 2017. Its seismic design regulations define minimum standards for buildings that exceed a certain size based on their floor counts or floor areas (Table 1). In addition, the Building Act generally categorizes buildings constructed over 30 years ago as “old buildings” at greater risk of collapse. We assumed that buildings in Gyeongju exempted from the seismic design regulations, and buildings over 30 years old, presented risks for collapse in our hypothetical earthquake disaster. In our study area, 11,819 buildings (61.2%) fell within these categories. We estimated building heights by multiplying the number of floors by an assumed floor-to-floor height of 3 m.

Table 1. Seismic design regulations by year in South Korea. For example, buildings with two or more stories or areas larger than 200 m² have had to be constructed with seismic designs since 2018.

Revision Year	1990	2005	2015	2017	2018
Minimum number of floors	6	3	3	2	2
Minimum floor area (m ²)	10,000	1000	500	500	200

The Korea National Disaster Management Institute models the potential hazard area of building collapse as anywhere within a distance 1.5 times the building's height [2]. We adopted this approach and drew buffers based on this distance around each building (Figure 2).

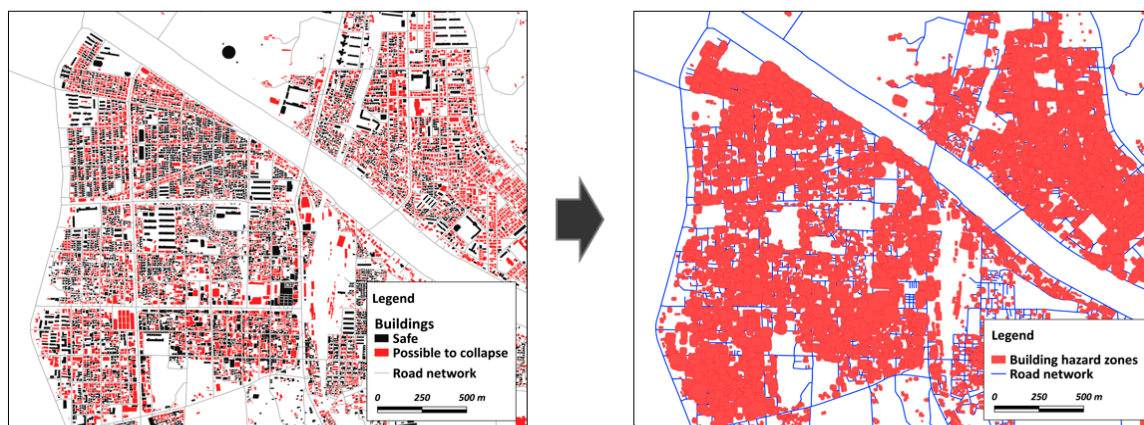


Figure 2. Building collapse estimation. The inner spaces of the main districts in Gyeongju with many old buildings become riskier, while the outer roads are relatively safe.

Next, we estimated potential road hazards using the estimated building collapse zones. We calculated “road hazard” using the length of the intersection of road segments and the proportional overlap with building collapse hazard zones (Figure 3).

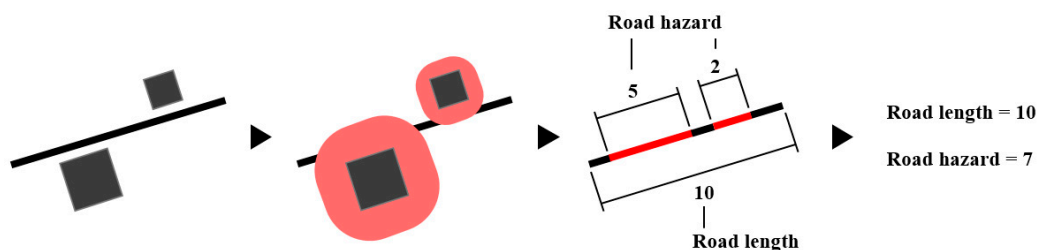


Figure 3. Road hazard analysis.

2.3. Pedestrian Evacuation Route Analysis

We used four approaches to validate the efficiency of our evacuation route analysis method: (1) a shortest-path, unassigned-shelter analysis that does not guide pedestrians to any particular shelter; (2) a shortest-path, assigned-shelter analysis calculating the minimum distance while considering shelter capacity; (3) a minimum-hazard, assigned-shelter analysis minimizing exposure to road hazards; and (4) our proposed method, a comprehensive evacuation route analysis seeking to minimize both distance and hazard. Our proposed evacuation route analysis model was applied and run as a Python script with GDAL and NetworkX libraries, and the evacuation routes were exported in shapefiles readable using QGIS, a GIS software tool. The key variables for evacuation route analysis are summarized in Table 2:

Table 2. Key variables for evacuation route analysis.

	Symbol	Description	Approach
Distance	$E_d(i)$	Road distance of edge i	Shortest-path, unassigned-shelter analysis Shortest-path, assigned-shelter analysis Comprehensive evacuation route analysis
Hazard	$E_h(i)$	Road hazard of edge i	Minimum-hazard, assigned-shelter analysis Comprehensive evacuation route analysis
Population	P_i	Number of population in node i	All approaches
Capacity	C_j	Population that can enter shelter j in its remaining space	All approaches

2.3.1. Shortest-Path, Unassigned-Shelter Analysis

The shortest-path, unassigned-shelter analysis (SUA) assumes that citizens receive no instructions on which shelter to go to after the earthquake. The only information they have is the shelter locations and the road network. In the model, each individual evacuates to the nearest shelter along the shortest available path through the road network. We modeled the natural evacuation pattern for an earthquake disaster in Gyeongju in this way, because Korean disaster management planning does not currently assign or communicate evacuation routes to shelters. The result reflects the best-case scenario if all pedestrians took the shortest paths to their nearest shelters, and we would expect the evacuation routes in actual earthquake scenarios to be less efficient. A model of shortest path analysis is derived as follows:

$$\min \sum_{i \in R} E_d(i) \quad (1)$$

where i is the edge of the route and R is the route between the population node and shelter node. The model calculates the minimum distance path through the road network.

However, if someone arrives at a shelter that is already fully occupied, they must move to the next nearest shelter, and their evacuation distance increases. We assume a shelter capacity of 1 square meter per individual. This process is described below:

- Step 1: Identify the shortest path from population node i to shelter node j , where $P_i > 0$.
- Step 2: If $C_j = 0$, identify the shelter closest to this shelter j . Traverse the shortest path to that shelter, which becomes the new shelter j .
- Step 3: Repeat Step 2 until $C_j \neq 0$.
- Step 4: If $C_j \geq P_i$, assign P_i to the path. Next, $C_j = C_j - P_i$ and $P_i = 0$.
- Step 5: If $C_j < P_i$, assign $P_i - C_j$ to the path. Next, $C_j = 0$ and $P_i = P_i - C_j$.
- Step 6: If the sum of the populations or shelter capacities is zero, end the process. If not, return to Step 1.

2.3.2. The Shortest-Path, Assigned-Shelter Analysis

The shortest-path, assigned-shelter analysis (SAA) assigns shelters to citizens at the moment of the disaster. SAA calculates the shortest paths from populations to shelters as potential evacuation routes. In addition, SAA identifies which shelters will be at full capacity if everyone traveled to their nearest option and assigns excess populations to shelters that have remaining capacity. This differs from SUA in that individuals are guaranteed to have a spot available at their assigned shelter, preventing visits to multiple shelters and reducing the overall distance traveled. The process is described below:

- Step 1: Identify the shortest path from population node i to shelter node j , where $P_i > 0$ and $C_j > 0$.
- Step 2: If $C_j \geq P_i$, assign P_i to the path. Next, $C_j = C_j - P_i$ and $P_i = 0$.
- Step 3: If $C_j < P_i$, assign $P_i - C_j$ to the path. Next, $C_j = 0$ and $P_i = P_i - C_j$.
- Step 4: If the sum of populations or shelter capacities is zero, end the process. If not, return to Step 1.

2.3.3. Minimum-Hazard, Assigned-Shelter Analysis

The minimum-hazard, assigned-shelter analysis (MAA) calculates evacuation routes that minimize exposure to building collapse zones between populations and shelters. A model for minimizing road hazards is derived as follows:

$$\min \sum_{i \in R} E_h(i) \quad (2)$$

The model calculates paths that minimize the length of roads traveled that overlaps with building collapse zones, rather than considering the overall evacuation distances. The MAA process is structured similarly to SAA, but it uses E_h for the path cost in Step 1. The process is described below:

- Step 1: Identify the path that minimizes road hazards from population node i to shelter node j , where $P_i > 0$ and $C_j > 0$. If the paths to two or more shelters have the same road hazard exposure, we choose the shortest distance path.
- Step 2: If $C_j \geq P_i$, assign P_i to the path. Next, $C_j = C_j - P_i$ and $P_i = 0$.
- Step 3: If $C_j < P_i$, assign $P_i - C_j$ to the path. Next, $C_j = 0$ and $P_i = P_i - C_j$.
- Step 4: If the sum of the populations or shelter capacities is zero, end the process. If not, return to Step 1.

2.3.4. Comprehensive Evacuation Route Analysis

Comprehensive evacuation route analysis (CEA) is a heuristic path-finding model that attempts to minimize (1) the evacuation distance and (2) the road hazard exposure. Heuristic path finding is a practical approach to finding the best decision based on conflicting objectives within limited time [29–31]. Previous research proposed algorithms that optimize costs to calculate a single best solution for all objectives, by setting the maximum cost of each objective [29] or rank of objectives [31]. In this study, we propose a simple model to calculate evacuation routes balancing hazard exposure and walking distance.

The proposed model consists of two phases: the routing and assigning phase. In the routing phase, we calculate the path that minimizes the road hazards from each population node to every shelter. The pedestrians at that node can travel to any shelter but have only one route choice for each shelter. In the assigning phase, the model assigns populations to shelters based on which shelter is the closest along the pre-calculated route, while skipping shelters already at capacity. The process of the assigning phase is constructed in the same manner as SAA.

By separating process phases, the model mitigates the worse scenarios of the first two approaches. The routing phase guides pedestrians to safe paths by filtering out evacuation routes along which many road hazards would be encountered. The assigning phase sends people to the closest available shelter, while preventing unnecessary trips to fully occupied shelters. The processes are described below and in Figures 4 and 5:

Routing Phase

- Step 1: Calculate the paths that minimize the road hazards between the population nodes and shelter nodes.

Assigning Phase

- Step 2: Identify the shortest path from population node i to shelter node j , where $P_i > 0$ and $C_j > 0$.
- Step 3: If $C_j \geq P_i$, assign P_i to the path. Next, $C_j = C_j - P_i$ and $P_i = 0$.
- Step 4: If $C_j < P_i$, assign $P_i - C_j$ to the path. Next, $C_j = 0$ and $P_i = P_i - C_j$.
- Step 5: If the sum of the populations or shelter capacities is zero, end the process. If not, iterate at Step 2.

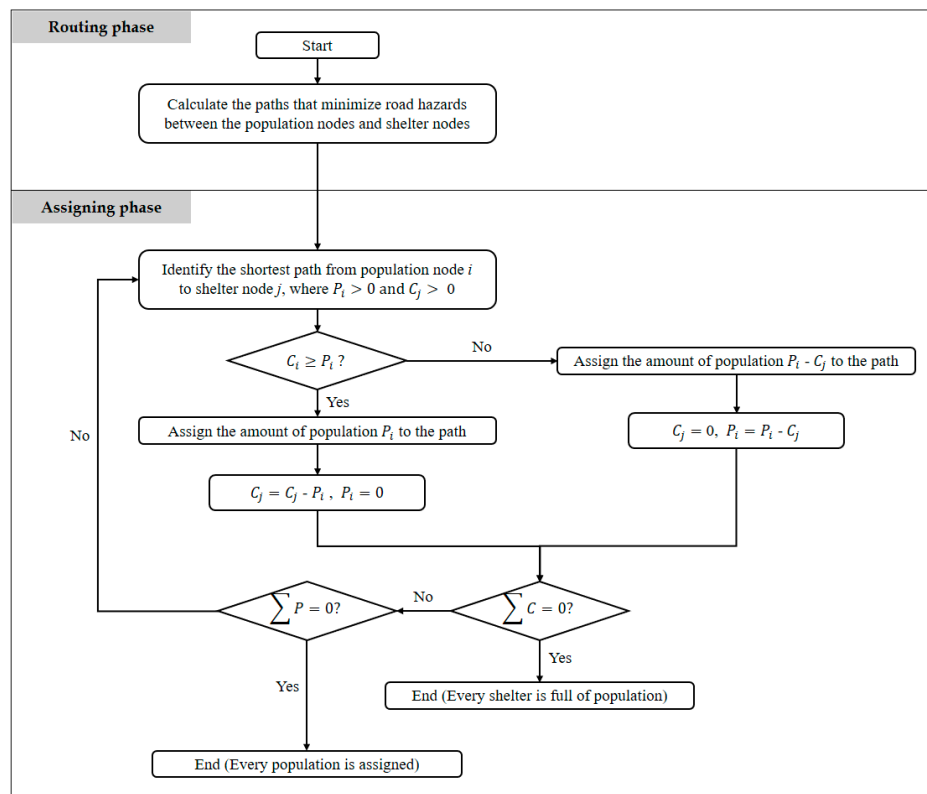


Figure 4. Process of comprehensive evacuation route analysis.

Population node	Shelter node	Evacuation distance	Distance rank	Road hazard	Hazard rank	
120	1	2,299.4	14	187.1	7	
120	2	439.5	20	170.5	8	CEA result
120	3	8,400.4	6	84.3	15	
120	4	1,247.1	19	84.3	15	
120	5	3,811.2	10	124.4	11	
120	6	12,296.7	1	147.2	9	
120	7	8,456.9	5	84.3	15	
120	8	3,264.4	13	439.2	2	
120	9	2,155.7	15	103.9	12	
120	10	1,817.4	18	221.4	6	
120	11	10,378.9	4	91.5	14	
120	12	1,953.6	16	84.3	15	
120	13	12,183.5	2	92.7	13	
120	14	4,694.0	8	457.4	1	
120	15	3,951.9	9	358.1	3	
120	16	7,609.7	7	131.1	10	
120	17	3,281.6	12	288.9	4	
120	18	10,903.3	3	84.3	15	
120	19	1,949.0	17	280.6	5	
120	20	3,795.3	11	84.3	15	MAA result

Population node	Shelter node	Evacuation distance	Distance rank	Road hazard	Hazard rank	
120	2	414.3		408.7		SUA&SAA result

Figure 5. Example of evacuation route results. The first table shows routes filtered by the routing phase of comprehensive evacuation route analysis (CEA). Minimum-hazard, assigned-shelter analysis (MAA) selects a route minimizing road hazards (the first two shortest paths are not selected due to fully occupied shelters). CEA selects a route with a lower evacuation distance than the MAA route. Although this route is longer than the shortest-path, unassigned-shelter analysis (SUA)/SAA routes, it results in significantly less hazard exposure.

3. Experimental Results

3.1. Summary of Results

In this section, we summarize four evacuation route analysis methods for Gyeongju. The summarized results are presented in Tables 3 and 4, and Figure 6. A two-sample *t*-test was applied in order to examine the coincidence between each method.

Table 3. Summary of results of evacuation route analysis.

Analysis Type	Evacuation Distance (m)			Hazard Exposure (m)		
	Mean	Std.	Max	Mean	Std.	Max
SUA	612.5	464.5	2625.4	306.1	224.7	2147.0
SAA	608.3	460.8	2485.8	303.0	220.3	1792.5
MAA	4991.5	4745.0	16,270.0	168.4	123.8	628.4
CEA	861.2	964.9	5759.5	199.5	141.2	703.4

Table 4. Two-sample *t*-test results for evacuation route analysis.

Analysis Type	Evacuation Distance	Hazard Exposure
	Two Sample <i>t</i> -Test (<i>t</i>)	Two Sample <i>t</i> -Test (<i>t</i>)
SUA vs. SAA	0.308	0.878
SUA vs. MAA	−348.089 ***	183.961 ***
SUA vs. CEA	−107.479 ***	137.785 ***
SAA vs. MAA	−348.129 ***	182.947 ***
SAA vs. CEA	−107.704 ***	136.777 ***
MAA vs. CEA	324.555 ***	−60.000 ***

*** $p < 0.001$.

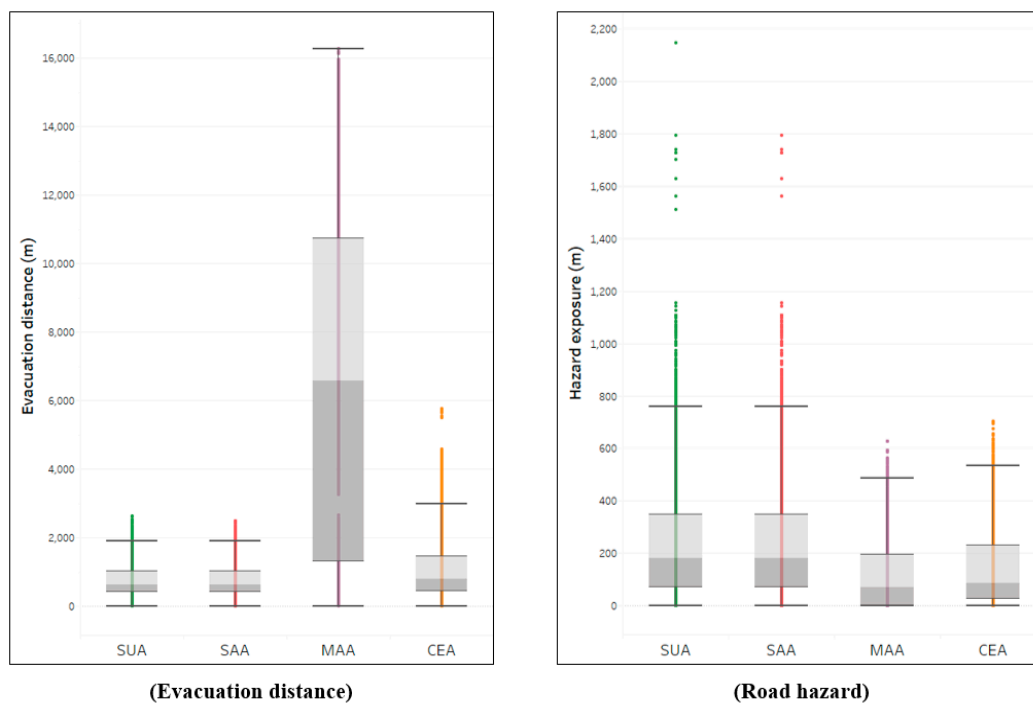


Figure 6. Evacuation distance and road hazard for each route analysis.

3.2. Model Comparison

Figures 7 and 8 illustrate the evacuation routes and hazard exposure for each route analysis. As shown in Tables 3 and 4, SAA reduced the average evacuation distance and hazard exposure compared with SUA, since it directly assigned pedestrians to empty shelters, but the differences were not statistically significant ($p > 0.05$). Although both SUA and SAA provided shorter evacuation routes than the other two approaches, these paths included more road hazards. In particular, these road hazards were concentrated in the three main districts that contained most of the population (Figures 1 and 8). As the box plots in Figure 5 show, some outliers of hazard exposure were significantly high. In the worst case, pedestrians would have to walk 2.2 km through building collapse zones while evacuating.

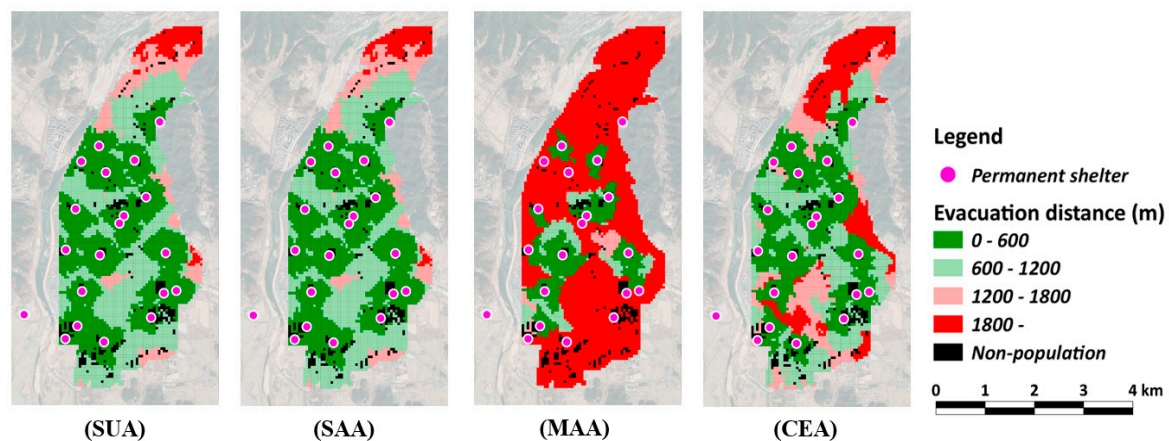


Figure 7. Evacuation distance for each route analysis.

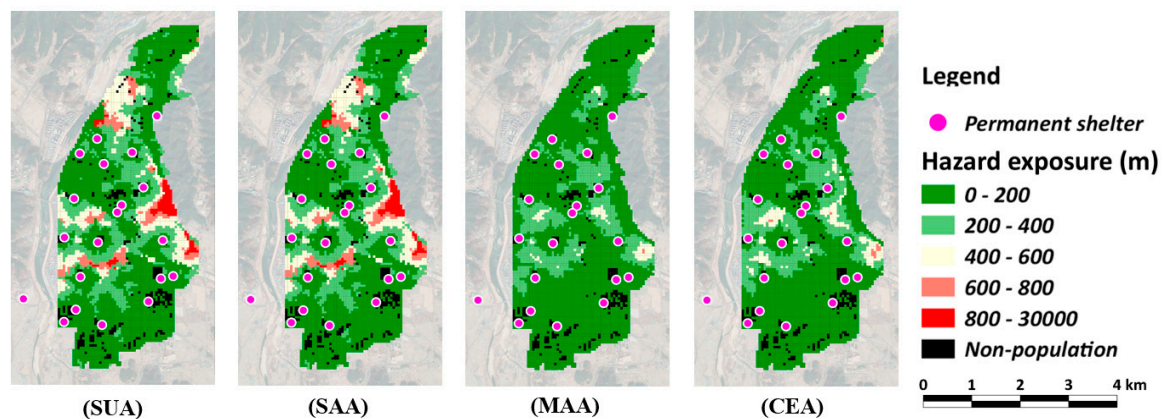


Figure 8. Road hazard for each route analysis.

MAA greatly reduced road hazards more than the other three approaches; there were statistically significant differences in hazard exposure between the routes from MAA and the others ($p < 0.001$). However, it also greatly increased the evacuation distance (by ~720% more on average than SAA, $p < 0.001$) since it did not attempt to minimize the overall route distances. The average evacuation distance was ~5 km, implying an 83-min trip at a 1 m/s walking speed.

Although there was significantly greater road hazard exposure for CEA than MAA ($p < 0.001$), there was also significantly less exposure with CEA than with SUA and SAA ($p < 0.001$). Furthermore, CEA reduced the average overall evacuation distance by ~83% compared to MAA ($p < 0.001$). Although this was still longer than that with SUA, CEA eliminated the high-risk outliers for hazard exposure seen with SAA (Figure 6). This approach helped pedestrians to avoid long and dangerous roads.

4. Discussion

Our suggested method, CEA, significantly reduced the hazard exposure compared to the shortest path calculations. While there are some trade-offs in forcing longer trips in order to avoid high-risk areas, the comprehensive approach mitigates this problem by selecting shorter routes from a subset of risk-minimizing options.

Figure 9 illustrates examples of evacuation routes for each approach. In the SUA and SAA examples, most evacuees travel through the central districts of the city, saving time but with high exposure to risks from the dense built environment. Many older, historic buildings are in the main districts of Gyeongju, where roads are more likely to be blocked or dangerous after an earthquake. As shown in Figure 7, long hazard exposures were concentrated in three main districts, where much of the floating population was located. In general, pedestrians walked further in scenarios of SUA than in those of SAA, because they had to continue walking from shelter to shelter until they found one that was not fully occupied. However, the evacuation distance gap between SUA and SAA was not high because the shelters were not very far from each other in the study area.

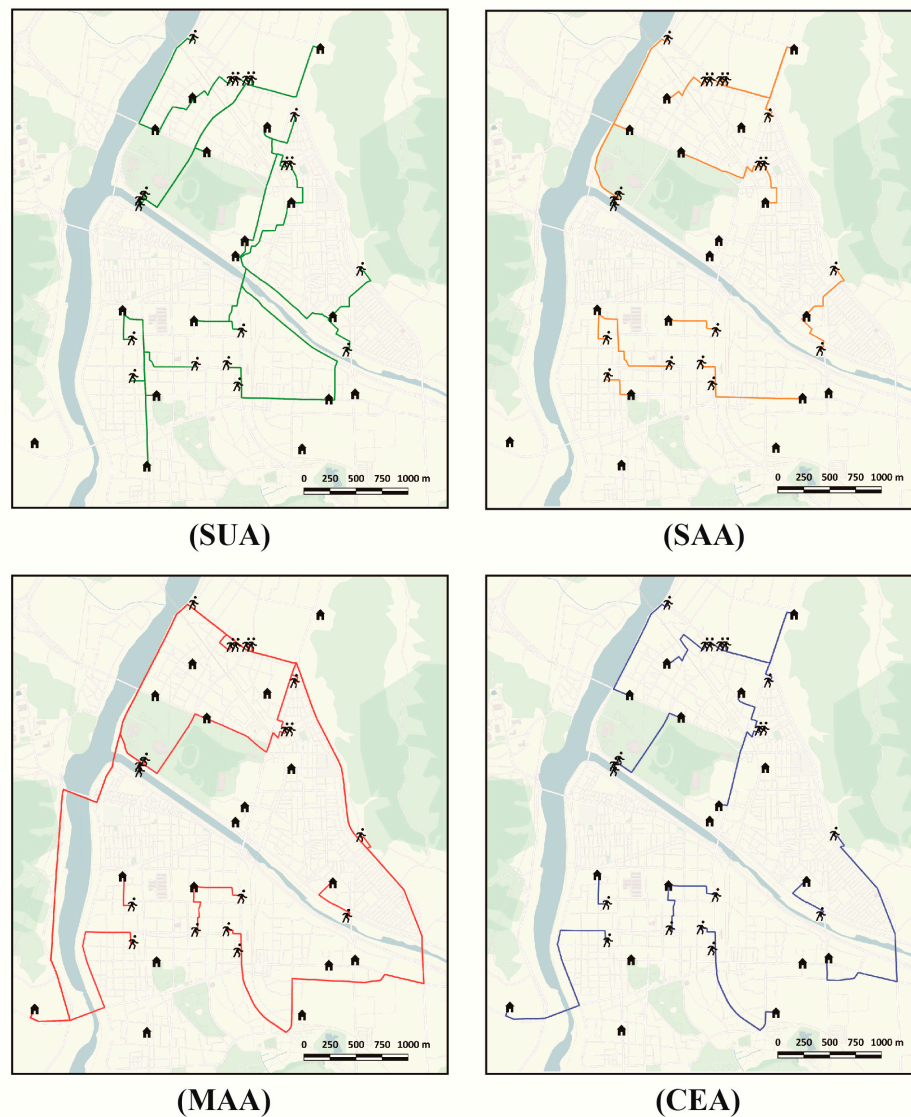


Figure 9. Examples of route change for each analysis. SAA provides more direct paths to shelters than SUA, by eliminating trips to multiple shelters. Pedestrians mostly use outer roads through MAA. CEA navigates pedestrians to shelters via safe routes that have reasonable walking distances.

In the MAA results, the evacuees stuck to outer roads; even when they walked through central districts, they used roads adjoining large open spaces such as parks and public stadia. In addition, the boundary of our study site borders rivers, farms, and hilly areas, which—while sparsely populated—have well-developed pedestrian pathways that connect many of Gyeongju’s historic attractions. MAA guided pedestrians to walk along these safe routes. However, this forced some evacuees to walk long distances to shelters. Some users may not be physically capable of walking for two hours to reach the nearest shelter.

CEA prevents pedestrians from walking extreme distances to shelters, by striking a balance between safety and proximity. In particular, it significantly reduced the hazard exposures in the main districts of Gyeongju (Figure 7), and many evacuees were guided away from building collapse zones. They prevented the crossing of the riskiest districts while selecting routes with reasonable evacuation distances and low-to-moderate risk exposure. Although CEA significantly reduced the hazard exposures of the evacuation routes, some pedestrians would walk farther than the shortest paths. In Figure 6, the evacuation routes in three regions significantly increased (Northern, Southern, and Eastern parts of the study site). We can suggest the designation of additional shelters in order to reduce the evacuation distances in these regions. Our proposed approach is able to find vulnerable areas and improve the efficiency of evacuation routes in disaster management planning for earthquakes.

The future research directions are to apply various pedestrian safety indicators to our evacuation route analysis and to study how proactive evacuation plans would change as floating population distributions change hour-to-hour and day-to-day. We can also improve on our routing optimization methods; all the methods we applied here were greedy heuristics, minimizing the costs for each node individually in some order, without attempting to optimize globally for all the nodes in aggregate. In addition, because we handled hourly updated floating population data and the proposed method was designed to calculate evacuation routes within one hour, our method could afford to run more slowly than real-time. However, we can improve this performance so that it operates faster than real-time.

Looking beyond building collapse as the main risk to evacuees, we can incorporate other risk factors such as gas explosions or ground displacement, allowing for more realistic plans during earthquake disasters. By capturing floating population distributions frequently from mobile phone networks, we can better measure and inform evacuation plans. Our available floating population data did not include population characteristics such as age and gender or ways in which to distinguish between local residents and visitors, or those with mobility challenges. Other studies have modeled evacuation routes considering the physical characteristics of populations [32] or simulated evacuation behaviors for different population groups [33].

5. Conclusions

In this study, we demonstrated how we can take pedestrian safety risks into account in evacuation planning. We proposed an approach for routing people to permanent shelters, considering exposure to the risk of earthquake building collapse. We modeled these risks by estimating building collapse hazard zones and incorporating them as travel costs of traversing the path network in Gyeongju. We used a heuristic path-finding approach to calculate the evacuation routes minimizing evacuation distance and hazard exposure. Our results showed that it is feasible to balance both safety and expediency using this comprehensive approach.

We believe that our study shows the potential value and limitations of evacuation planning when incorporating safety indicators into route analysis. Earthquake risk assessment is complex and can include many options to consider, such as building collapse or gas explosions. We can improve our plans by quantifying these risks in collaboration with disaster-related experts and can help citizens to increase their survival rate in disaster situations. Our results are not a final statement on evacuation planning but a first step toward safer, responsive, and efficient evacuation routes during earthquake disasters.

Author Contributions: Conceptualization, Wonjun No, Junyong Choi, Sangjoon Park, and David Lee; methodology, Wonjun No, Junyong Choi, Sangjoon Park, and David Lee; data curation, Wonjun No and Sangjoon Park; validation, Wonjun No, Junyong Choi, and David Lee; visualization, Wonjun No; writing—original draft, Wonjun No; writing—review and editing, Junyong Choi and David Lee; supervision, David Lee; project administration, David Lee; funding acquisition, David Lee. All authors have read and agreed to the published version of the manuscript.

Funding: This research was supported by a grant (20TSRD-B151228-02) from the Urban Declining Area Regenerative Capacity-Enhancing Technology Research Program funded by the Ministry of Land, Infrastructure and Transport of the South Korean government.

Conflicts of Interest: The authors declare no conflict of interest.

References

1. Grigoli, F.; Cesca, S.; Rinaldi, A.P.; Manconi, A.; Lopez-Comino, J.A.; Clinton, J.F.; Westaway, R.; Cauzzi, C.; Dahm, T.; Wiemer, S. The November 2017 Mw 5.5 Pohang Earthquake: A Possible Case of Induced Seismicity in South Korea. *Science* **2018**, *360*, 1003–1006. [[CrossRef](#)] [[PubMed](#)]
2. Lee, J.; Son, M.; Park, D.; Jung, T.; Lee, B.; Kim, D.; Lim, K.; Park, K.; Kang, H.; Han, S. *Development on Designation and Operation Standard of Earthquake Evacuation Shelter*; Technical Report on PRI-2017-02-01-01; Korean National Disaster Management Research Institute: Ulsan, Korea, 2017.
3. D’Orazio, M.; Spalazzi, L.; Quagliarini, E.; Bernardini, G. Agent-Based Model for Earthquake Pedestrians’ Evacuation in Urban Outdoor Scenarios: Behavioural Patterns Definition and Evacuation Paths Choice. *Saf. Sci.* **2014**, *62*, 450–465. [[CrossRef](#)]
4. Yang, Q.; Sun, Y.; Liu, X.; Wang, J. MAS-Based Evacuation Simulation of an Urban Community during an Urban Rainstorm Disaster in China. *Sustainability* **2020**, *12*, 546. [[CrossRef](#)]
5. Campos, V.; Bandeira, R.; Bandeira, A. A Method for Evacuation Route Planning in Disaster Situations. *Procedia Soc. Behav. Sci.* **2012**, *54*, 503–512. [[CrossRef](#)]
6. Wood, N.J.; Schmidtlein, M.C. Anisotropic Path Modeling to Assess Pedestrian-Evacuation Potential from Cascadia-Related Tsunamis in the US Pacific Northwest. *Nat. Hazards* **2012**, *62*, 275–300. [[CrossRef](#)]
7. Cova, T.J.; Church, R.L. Modelling Community Evacuation Vulnerability Using GIS. *Int. J. Geogr. Inf. Sci.* **1997**, *11*, 763–784. [[CrossRef](#)]
8. Opananon, S.; Miller-Hooks, E. The Safest Escape Problem. *J. Oper. Res. Soc.* **2009**, *60*, 1749–1758. [[CrossRef](#)]
9. Lämmel, G.; Klüpfel, H.; Nagel, K. Risk Minimizing Evacuation Strategies under Uncertainty. In *Pedestrian and Evacuation Dynamics*; Springer: Berlin/Heidelberg, Germany, 2011; pp. 287–296.
10. Xu, J.; Yin, X.; Chen, D.; An, J.; Nie, G. Multi-Criteria Location Model of Earthquake Evacuation Shelters to Aid in Urban Planning. *Int. J. Disaster Risk Reduct.* **2016**, *20*, 51–62. [[CrossRef](#)]
11. Lee, Y.L.; Ishii, H.; Tai, C.A. Earthquake Shelter Location Evaluation Considering Road Structure. *Int. Conf. Intell. Syst. Des. Appl. ISDA* **2008**, *1*, 495–497. [[CrossRef](#)]
12. Ndiaye, I.A.; Neron, E.; Linot, A.; Monmarche, N.; Goerigk, M. A New Model for Macroscopic Pedestrian Evacuation Planning with Safety and Duration Criteria. *Transp. Res. Procedia* **2014**, *2*, 486–494. [[CrossRef](#)]
13. Zhang, N.; Huang, H.; Su, B.; Zhao, J. Analysis of Dynamic Road Risk for Pedestrian Evacuation. *Phys. A Stat. Mech. Its Appl.* **2015**, *430*, 171–183. [[CrossRef](#)]
14. Yamamoto, K.; Li, X. Safety Evaluation of Evacuation Routes in Central Tokyo Assuming a Large-Scale Evacuation in Case of Earthquake Disasters. *J. Risk Financ. Manag.* **2017**, *10*, 14. [[CrossRef](#)]
15. Zhao, X.; Du, P.; Chen, J.; Yu, D.; Xu, W.; Lou, S.; Yuan, H.; Ip, K.P. A Typhoon Shelter Selection and Evacuee Allocation Model: A Case Study of Macao (SAR), China. *Sustainability* **2020**, *12*, 3308. [[CrossRef](#)]
16. Li, J.; Zhu, H. A Risk-Based Model of Evacuation Route Optimization under Fire. *Procedia Eng.* **2018**, *211*, 365–371. [[CrossRef](#)]
17. El Meouche, R.; Abunemeh, M.; Hijaze, I.; Mebarki, A.; Shahrour, I. Developing Optimal Paths for Evacuating Risky Construction Sites. *J. Constr. Eng. Manag.* **2018**, *144*, 4017099. [[CrossRef](#)]
18. Chen, P.; Chen, G.; Wang, L.; Reniers, G. Optimizing Emergency Rescue and Evacuation Planning with Intelligent Obstacle Avoidance in a Chemical Industrial Park. *J. Loss Prev. Process Ind.* **2018**, *56*, 119–127. [[CrossRef](#)]
19. Dijkstra, E.W. A Note on Two Problems in Connexion with Graphs. *Numer. Math.* **1959**, *1*, 269–271. [[CrossRef](#)]

20. Kim, Y.; Rhie, J.; Kang, T.-S.; Kim, K.-H.; Kim, M.; Lee, S.-J. The 12 September 2016 Gyeongju Earthquakes: 1. Observation and Remaining Questions. *Geosci. J.* **2016**, *20*, 747–752. [CrossRef]
21. Son, M.; Cho, C.S.; Shin, J.S.; Rhee, H.; Sheen, D. Spatiotemporal Distribution of Events during the First Three Months of the 2016 Gyeongju, Korea, Earthquake Sequence. *Bull. Seismol. Soc. Am.* **2018**, *108*, 210–217. [CrossRef]
22. Korean Statistical Information Service. Earthquake Statistics. Available online: <http://kosis.kr/index/index.do> (accessed on 20 April 2020).
23. Korea National Spatial Infrastructure Portal. Available online: <http://data.nsdi.go.kr/dataset/20180927ds0062> (accessed on 15 March 2020).
24. Korea Ministry of Public Administration and Security. Korea Road Name Address System Website. Available online: <http://www.juso.go.kr/> (accessed on 10 March 2019).
25. Korea National Public Data Portal. Available online: <https://www.data.go.kr/data/15021030/openapi.do> (accessed on 15 March 2020).
26. Pei, T.; Sobolevsky, S.; Ratti, C.; Shaw, S.-L.; Li, T.; Zhou, C. A New Insight into Land Use Classification Based on Aggregated Mobile Phone Data. *Int. J. Geogr. Inf. Sci.* **2014**, *28*, 1988–2007. [CrossRef]
27. Gyeongju. Gyeongju Population Status. Available online: http://www.gyeongju.go.kr/open_content/ko/page.do?mnu_uid=292&parm_mnu_uid=1592&srchBgpUid=590 (accessed on 10 May 2020).
28. Lu, X.; Yang, Z.; Cimellaro, G.P.; Xu, Z. Pedestrian Evacuation Simulation under the Scenario with Earthquake-Induced Falling Debris. *Saf. Sci.* **2019**, *114*, 61–71. [CrossRef]
29. Wakuta, K. A Multi-Objective Shortest Path Problem. *Math. Methods Oper. Res.* **2002**, *54*, 445–454. [CrossRef]
30. Sastry, V.N.; Janakiraman, T.N.; Mohideen, S.I. New Algorithms For Multi Objective Shortest Path Problem. *Opsearch* **2003**, *40*, 278–298. [CrossRef]
31. Wang, S.; Yang, J.; Liu, G.; Du, S.; Yan, J. Multi-Objective Path Finding in Stochastic Networks Using a Biogeography-Based Optimization Method. *Simulation* **2016**, *92*, 637–647. [CrossRef]
32. Mayasari, Z.M.; Rafflesia, U.; Astuti, M.; Fauzi, Y. Mathematical Modeling Approach of an Evacuation Model for Tsunami Risk Reduction in Bengkulu. In *Journal of Physics: Conference Series*; IOP Publishing: Yogyakarta, Indonesia, 2019; Volume 1188, p. 12094.
33. Takabatake, T.; Shibayama, T.; Esteban, M.; Ishii, H.; Hamano, G. Simulated Tsunami Evacuation Behavior of Local Residents and Visitors in Kamakura, Japan. *Int. J. Disaster Risk Reduct.* **2017**, *23*, 1–14. [CrossRef]



© 2020 by the authors. Licensee MDPI, Basel, Switzerland. This article is an open access article distributed under the terms and conditions of the Creative Commons Attribution (CC BY) license (<http://creativecommons.org/licenses/by/4.0/>).